Snapin-Mediated BACE1 Retrograde Transport Is Essential for Its Degradation in Lysosomes and Regulation of APP Processing in Neurons

Xuan Ye[1] and Qian Cai[1,*]

[1]Department of Cell Biology and Neuroscience, Nelson Biological Laboratories, Rutgers University, Room B231, 604 Allison Road, Piscataway, NJ 08854, USA

*Correspondence: cai@biology.rutgers.edu

SUMMARY

β site amyloid precursor protein (APP)-cleaving enzyme 1 (BACE1) is the major β secretase for generating β-amyloid (Aβ) peptides. The acidic environment of endosomes is optimal for β secretase activity. However, the mechanisms regulating BACE1 traffic from endosomes to lysosomes for degradation are largely unknown. Here, using snapin-deficient mice combined with gene rescue experiments, we reveal that Snapin, as a dynein motor adaptor for late endosomes, mediates BACE1 retrograde transport. hAPP mutant live neurons and mouse brains exhibited BACE1 accumulation within the altered late endocytic organelles and defective lysosomal targeting due to reduced Snapin-dynein coupling. Deleting snapin or disrupting Snapin-dynein coupling reduces BACE1 transport to lysosomes for degradation, thus enhancing APP processing. Overexpressing Snapin in hAPP neurons reduces β site cleavage of APP by enhancing BACE1 turnover. Altogether, our study provides mechanistic insights into the complex regulation of BACE1 level and activity and turnover through retrograde transport, thus controlling Aβ generation in neurons.

INTRODUCTION

Alzheimer's disease (AD) is characterized by the formation of senile plaques in patient brains (Hardy and Selkoe, 2002). The primary constituent of the senile plaques is β-amyloid (Aβ) peptide, which is generated by sequential proteolysis of amyloid precursor protein (APP) by β and γ secretases. β secretase is considered the initial and rate-limiting enzyme during this process (Vassar et al., 2009). β site APP-cleaving enzyme 1 (BACE1) is the major neuronal β secretase for Aβ generation (Vassar et al., 2009). The BACE1 level/activity increases with age (Fukumoto et al., 2004) and is elevated in AD patient brains

(Yang et al., 2003), making BACE1 a prime target for therapeutic intervention. BACE1 is a single-membrane spanning protease and delivered to the cell surface from the trans-Golgi network (TGN). The trafficking of BACE1 to endosomes is thought to occur via internalization from the plasma membrane, or directly from the TGN (Huse et al., 2000; Sannerud et al., 2011; Kang et al., 2012; Prabhu et al., 2012). Late endosomes or multivesicular bodies (MVBs) provide an acidic environment necessary for optimal β secretase activity (Huse et al., 2000; Tesco et al., 2007; Sannerud et al., 2011; Wu et al., 2011). BACE1 ultimately undergoes degradation in lysosomes (Tesco et al., 2007; Lefort et al., 2012). Thus, the BACE1 traffic route from endosomes to lysosomes is critical to control its level and activity. However, the mechanism regulating the delivery of BACE1 to lysosomes in neurons remains largely unknown.

Alterations in the endosome-lysosome trafficking and Aβ accumulation within endosomes are among the earliest findings in AD brains (Nixon, 2005; Ginsberg et al., 2010). Late endosomes containing Aβ42 are clustered in distal processes and synaptic terminals in mutant hAPP transgenic (Tg) mice (Takahashi et al., 2002, 2004). The amount of pathogenic Aβ in the brain depends on the BACE1 level and its β secretase activity. Amyloidogenic processing of APP appears to occur preferentially in endosomes (Haass et al., 1992; Koo and Squazzo, 1994; Takahashi et al., 2004; Wu et al., 2011), raising a fundamental question: can the altered endosomal-lysosomal system in AD neurons contribute to Aβ accumulation by changing BACE1 level and its β secretase activity? In current study, we reveal that hAPP mutant live neurons and mouse brains exhibited an aberrant BACE1 accumulation within the altered late endocytic organelles due to its defective lysosomal targeting. These phenotypes are attributable to a reduced coupling of dynein motor to its adaptor Snapin for driving retrograde transport of BACE1-cargo late endosomes. Deleting snapin or disrupting Snapin-dynein coupling reduces BACE1 transport to lysosomes for degradation, thus enhancing APP processing. Overexpressing Snapin in hAPP neurons reduces β site cleavage of APP by enhancing BACE1 turnover. Thus, our study reveals a cellular pathway that dynamically regulates the balance between BACE1 transport/turnover and APP processing, thereby advancing our knowledge that may be essential for controlling Aβ generation relevant to AD pathogenesis.
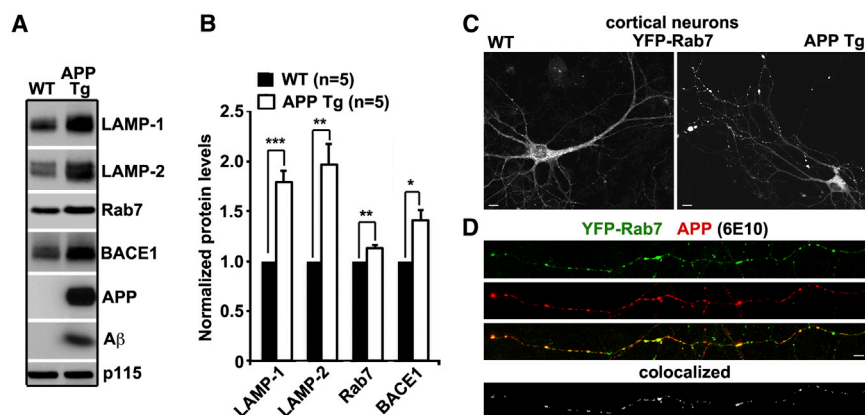
Figure 1. Accumulation of APP and BACE1 within Late Endosomes in Mutant hAPP Neurons

(A and B) Representative blots (A) and quantitative analysis (B) showing accumulation of BACE1 along the altered late endocytic pathway in the brain of hAPP mutant Tg mice. A total of 20 μg of brain homogenates from WT and hAPP Tg mice was sequentially detected on the same membrane. Relative protein levels were normalized by p115 and to that of WT littermates. Data were analyzed from five pairs of mice for each genotype and expressed as mean ± SEM with Student's t test: ***$p < 0.001$; **$p < 0.01$; *$p < 0.05$.

(C) Representative images showing distribution patterns of Rab7-labeled late endosomes in cultured cortical neurons from WT and hAPP mutant Tg (J20) mice. Neurons were transfected with YFP-Rab7 at 6 DIV and imaged at 9 DIV. Note that late endosomes in hAPP mutant neurons appear as large clusters along neuronal processes, particularly in distal regions.

(D) Representative axonal images showing late endosomal targeting of APP or its cleaved products (C99 and Aβ) in APP mutant neurons with colocalized puncta. Neurons were transfected at 6 DIV and coimmunostained with MAP2 and 6E10 antibodies at 16 DIV. MAP2-negative axons were selected for imaging.

Scale bars represent 10 μm (C and D). See also Figure S1.

RESULTS

Accumulation of APP and BACE1 within Late Endosomes in Mutant hAPP Neurons

We first performed sequential immunoblots of brain cortex homogenates from wild-type (WT) and hAPP Tg mice harboring the human AD Swedish and Indiana mutations (CaMKIIα-tTA X tet-APPswe/ind) (Jankowsky et al., 2005) (Figure 1A). Increased intensity of lysosomal-associated membrane protein 1 (LAMP-1), LAMP-2, Rab7, and BACE1 was consistently observed in hAPP mutant Tg mouse brains, whereas the Golgi marker p115 level exhibited no detectable change (Figure 1B). These results indicate an altered late endocytic system accompanied with an increased BACE1 level in hAPP Tg mice. BACE1 mRNA levels show no significant increase in hAPP Tg mouse cortices (Figures S1A and S1B), suggesting that the observed change in BACE1 steady-state levels is likely attributed to its slower turnover rate, rather than elevated BACE1 expression.

We next compared the distribution patterns of late endosomes labeled by YFP-Rab7 in cortical neurons cultured from WT and hAPP Tg mice harboring the human AD Swedish and Indiana mutations (J20) (Mucke et al., 2000). In WT neurons, late endosomes appeared as small and fine vesicular structures uniformly distributed along neuronal processes. Surprisingly, late endosomes in hAPP Tg neurons were clustered as larger puncta at distal processes (Figure 1C), suggesting an impaired late endocytic trafficking. Coimmunostaining assay showed that a majority of C99/Aβ or APP, detected by a β amyloid (6E10) antibody, was colocalized with late endosomes along MAP2-negative distal axons in mutant hAPP neurons (Figure 1D). Consistently, late endosomes in neurons expressing hAPPswe appeared to be clustered at distal processes (Figure S1C). Although hAPP can be readily detected within late endocytic organelles, expressing hAPPswe increased retention of APP or its cleaved products within late endosomes by ~3.4-fold ($p < 0.001$) (Figures S1D and S1E). BACE1 and APP were largely colocalized as

vesicular structures within axons (Figure S1H). Our data suggest that hAPP mutant expression in neurons induces defects in late endocytic trafficking, which further increases APP processing by reducing BACE1 turnover.

Impaired BACE1 Retrograde Transport in hAPP Tg Neurons

We next asked whether BACE1 associates with Rab7-labeled late endosomes moving along axons of mature neurons. Time-lapse imaging in live neurons showed that a majority of BACE1 was targeted to late endosomes, some of which comigrated from the distal axon toward the soma (Figure 2A), supporting a hypothesis that BACE1 utilizes late endosomes as cargo carrier for its traffic to mature lysosomes in the soma (Cai et al., 2010; Lee et al., 2011). Dynein is the major motor driving late endosomes for retrograde transport. We next examined the association of dynein motors with late endosomes by immunoisolation using Dyna magnetic beads coated with a Rab7 antibody. When equal amounts of late endocytic organelles were loaded as reflected by Rab7 levels, normalized intensity of the dynein intermediate chain (DIC) in hAPP mutant Tg mouse brains was significantly reduced to 27% in comparison with that of WT littermates ($p < 0.001$) (red box in Figures 2B and 2C), indicating a reduced loading of the dynein motors onto late endosomes. Snapin, as an adaptor, recruits dynein motors to late endosomes through Snapin-DIC coupling (Cai et al., 2010). Although Snapin levels display no detectable change ($p = 0.238$), reciprocal coimmunoprecipitation assays showed reduced Snapin-DIC coupling in hAPP Tg mouse brains. It suggests an impaired recruitment of dynein motors onto late endosomes. Snapin associated with Aβ, but not with mutant hAPP (Figure S2A; see the Supplemental Results).

Purified late endocytic organelles from hAPP Tg brains retained increased BACE1 ($p < 0.05$) relative to that from WT littermates (green box in Figure 2B). Moreover, hAPP mutant neurons exhibited reduced retrograde transport of late endosomes,
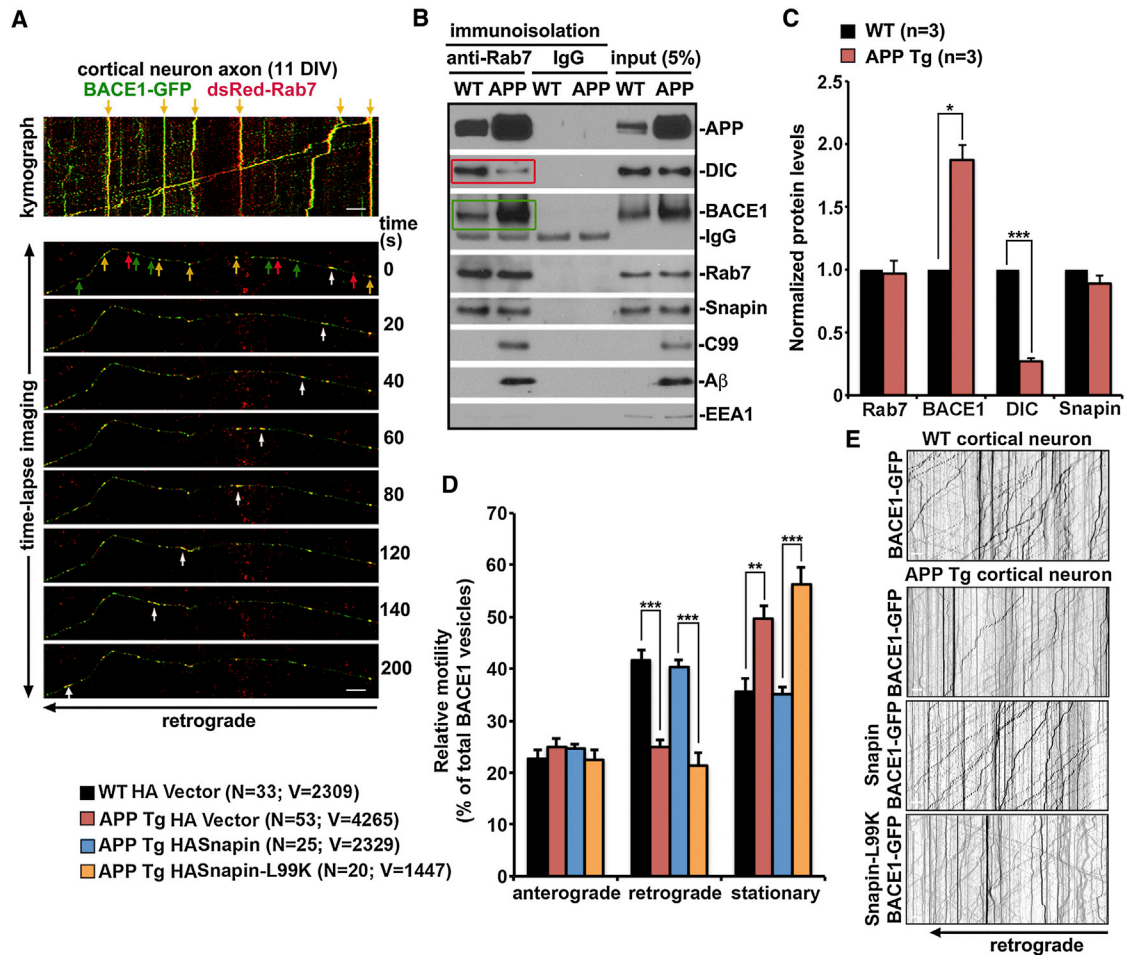
Figure 2. Impaired BACE1 Retrograde Transport in hAPP Tg Neurons

(A) Representative kymograph (upper) and time-lapse imaging (lower) showing colocalization (yellow) and comigration (white arrows) of BACE1 (green) and Rab7 (red) from the distal axon toward the soma of WT cortical neurons during a 200 s recording period. Neurons were transfected at 6 DIV, followed by time-lapse imaging at 11 DIV. The axon image was taken ~100 μm away from the cell body.

(B and C) Immunoisolation showing reduced dynein attachment to its cargo: late endosomes (in red box) containing robustly increased BACE1 (in green box) along with aberrant accumulation of APP, C99, and Aβ in hAPP Tg mouse brains. Rab7-associated organelles were immunoisolated with anti-Rab7-coated Dyna magnetic beads, followed by sequential immunoblotting on the same membranes after stripping between each antibody application. Data were quantified from three repeats.

(D and E) Quantitative analysis (D) and representative kymographs (E) showing impaired axonal retrograde transport of BACE1-GFP in hAPP mutant neurons (10–12 DIV), which is rescued by expressing Snapin, but not its L99K mutant defective in dynein DIC binding. Vertical lines represent stationary organelles, oblique lines or curves to the right (negative slope) represent anterograde movements, and lines to the left (positive slope) indicate retrograde transport. As an internal control, anterograde transport was not significantly altered along the same axons of APP mutant neurons. Data were quantified from a total number of axonal BACE1 vesicles (V) from a total number of neurons (N) in more than three experiments, as indicated in parentheses.

Scale bars represent 10 μm (A). Error bars represent SEM. Student's t test: ***p < 0.001; **p < 0.01; *p < 0.05. See also Figure S2 and Movies S1, S2, S3, and S4.

which can be rescued by overexpressing Snapin, but not its DIC-binding defective mutant (Figures S2B and S2C; see the Supplemental Results). We next examined whether retrograde transport of BACE1 is impaired in live hAPP mutant neurons. Similar to a previous report by Wang et al. (2012), BACE1 displayed dynamic bidirectional movement in WT neurons (anterograde, 22.66% ± 1.63%; retrograde, 41.81% ± 1.73%) (Figures 2D and 2E; Movie S1). In contrast, BACE1 in hAPP mutant cortical neurons showed selective defects in retrograde, but not anterograde, transport, thus increasing their stationary

pool (anterograde, 25.00% ± 1.44%; retrograde, 25.01% ± 1.40%; p < 0.001) (Figures 2D and 2E; Movie S2). Expressing Snapin, but not its L99K mutant defective in DIC binding in hAPP mutant neurons, rescued BACE1 retrograde transport (Snapin, 40.33% ± 1.28%; Snapin-L99K, 21.3% ± 2.58%) (Figures 2D and 2E; Movies S3 and S4).

Snapin-DIC Interaction Regulates APP Processing

We next asked whether a defective Snapin-DIC coupling causes an altered BACE1 distribution and motility, thus contributing to

the phenotypes observed in hAPP Tg neurons. In control neurons, BACE1 appeared as small and fine vesicular structures in dynamic and bidirectional movement (motility, 64.22% ± 3.63%; in which 25.50% ± 2.11% for anterograde and 38.72% ± 2.94% for retrograde) (Figures 3A and 3B; Movie S5). In contrast, *snapin* mutant cortical neurons from the *snapin flox* mice display reduced BACE1 retrograde transport (21.60% ± 1.98%; p < 0.001) with unaltered anterograde transport (Movie S6), resulting in larger clustering of BACE1 along distal processes. Reintroducing HA-Snapin into *snapin*-deficient neurons selectively recruited more stationary BACE1 vesicles into the retrograde motile pool (47.48% ± 1.54%; p = 0.0037) (Movie S7), highlighting a critical role for Snapin in mediating BACE1 retrograde transport in neurons. In addition, Snapin-DIC interaction is necessary for dynein-driven retrograde transport of BACE1 in neurons (Figures S3A and S3B; see the Supplemental Results).

We hypothesized that BACE1 retrograde transport is one of the important traffic pathways for its degradation in mature lysosomes in soma. It is supported by reduced colocalization mean intensity of BACE1-GFP with LAMP-1-mRFP in *snapin*-deficient neurons relative to WT controls (p < 0.001) (Figures 3C and 3D). S*napin* deficiency robustly increased BACE1 retention within late endocytic organelles in *snapin*[(−/−)] mouse embryonic fibroblasts (MEFs) (p < 0.0001) (Figures S3C and S3D); a phenotype could be reversed by expressing Snapin, but not its mutant Snapin-L99K. We next asked whether defective BACE1 transport in *snapin* mutant cells affects BACE1 degradation, thus enhancing APP processing. Deleting the *snapin* gene in mice displayed increased levels of endogenous BACE1 and APP-processing product CTFs in brain homogeneous (BACE1, p < 0.05; C99, p < 0.01; C89, p < 0.01; C83, p < 0.01) relative to their WT littermates (Figures 3E and 3F). Increased BACE1 and CTFs were consistently found in *snapin*[(−/−)] MEFs (Figure 3E). ELISAs in 1-month-old conditional *snapin*-deficient mice show dramatically increased Aβ in cerebral cortex and hippocampus (cortex: 188.96% ± 12.23%, p = 0.0054; hippocampus: 226.31% ± 15.2%, p = 0.0036) compared with their littermate controls (Figure 3G). These results indicate that Snapin-dynein-mediated endocytic transport controls Aβ production by enhancing BACE1 trafficking to lysosomes for turnover.

Snapin Reduces APP Processing in hAPP Tg Neurons

We next examined the distribution pattern of BACE1 in the hippocampal CA3 regions of the hAPP Tg mouse brains. In WT mice, whereas BACE1 signals appeared as vesicular structures in the soma-enriched areas, these signals were much weaker in the process-enriched areas. Conversely, distribution of BACE1 in hAPP Tg mouse brains is opposite: less BACE1 vesicular structures were found in the soma, and more BACE1 structures clustered and accumulated in distal processes. Averaged number of BACE1 clusters per section was substantially increased relative to WT controls (WT, 18.22 ± 3.50; hAPP Tg, 75.08 ± 7.80; p < 0.001) (Figure 4A). A majority of BACE1 clusters were colabeled by the 6E10 antibody, which detects both APP and its cleaved products C99 and Aβ deposits, accompanied by swollen/dystrophic neurites (Figure 4B).

To explore a mechanistic link between defects in BACE1 transport and its turnover through lysosomes, we examined lysosomal targeting of BACE1. BACE1 targeting to lysosomes was reduced by 50.29% ± 7.9% (p = 0.005) in hippocampal CA3 region of hAPP Tg mice in comparison with WT controls (Figure 4C). Consistently, BACE1 lysosomal targeting in cultured hAPP Tg neurons was similarly reduced to 55.26% ± 6.56% (Figure 4D). Our previous study demonstrates that elevated Snapin expression in neurons enhances late endocytic trafficking and lysosomal function (Cai et al., 2010). Thus, Snapin provides a potential molecular tool for accelerating BACE1 turnover and thereby reduces β site cleavage of APP. Overexpressing Snapin in COS7 cells reduces BACE1 and suppresses APP processing reflected by reduced APP-CTFs (Figure S4C). Consistently, elevated Snapin expression in hAPP Tg neurons by infection with Lenti-Snapin reduces both BACE1 and C99 to 70.04% ± 7.37% (p = 0.027) and 62.89% ± 2.26% (p = 0.004), respectively (Figures 4E and 4F). Furthermore, Snapin overexpression in *snapin*[(−/−)] MEFs effectively reduces BACE1 level, whereas disrupting Snapin-DIC coupling by expressing Snapin-L99K mutant increases BACE1 level (Figures S4A and S4B, see the Supplemental Results). These results suggest that Snapin-mediated retrograde transport facilitates BACE1 trafficking to lysosomes for degradation. Defects in BACE1 retrograde transport would retain BACE1 in the endocytic pathway within neurites, rather than being delivered to somatic mature lysosomes for degradation, thereby increasing APP processing and Aβ generation.

DISCUSSION

The amount of pathogenic Aβ peptide generated in the brain depends on the BACE1 level and its β secretase activity. Although the amyloidogenic processing of APP appears to preferentially occur in endosomes, BACE1 is degraded within lysosomal organelles (Tesco et al., 2007; Lefort et al., 2012) (Figure S4A). Thus, the traffic route for BACE1 from endosomes to lysosomes is critical to limiting its level and activity. Better understanding of the mechanisms regulating APP processing and BACE1 trafficking is crucial to dissecting the AD-associated pathological events.

Retrograde transport of late endosomes is crucial for the delivery of internalized proteins and target materials from distal processes to the soma where mature lysosomes are predominantly located (Cai et al., 2010; Lee et al., 2011). The mechanisms by which BACE1 is transported to lysosomes are not understood. Our current study provides mechanistic insights into the motor-adaptor machinery that drives BACE1 retrograde transport. Such a mechanism is critical for the regulation of BACE1 level and activity, thus controlling APP processing. We showed that hAPP Tg neurons and mouse brains exhibit defective BACE1 retrograde transport due to reduced Snapin-DIC coupling and impaired dynein motor loading onto late endosomes, thus leading to the aberrant accumulation of BACE1 and enhanced APP processing within late endosomal compartments along neuronal processes. We further demonstrated that Snapin acts as an adaptor selectively recruiting dynein motors to the BACE1-associated late endosomes. Snapin-mediated and dynein-driven retrograde transport is essential for the delivery
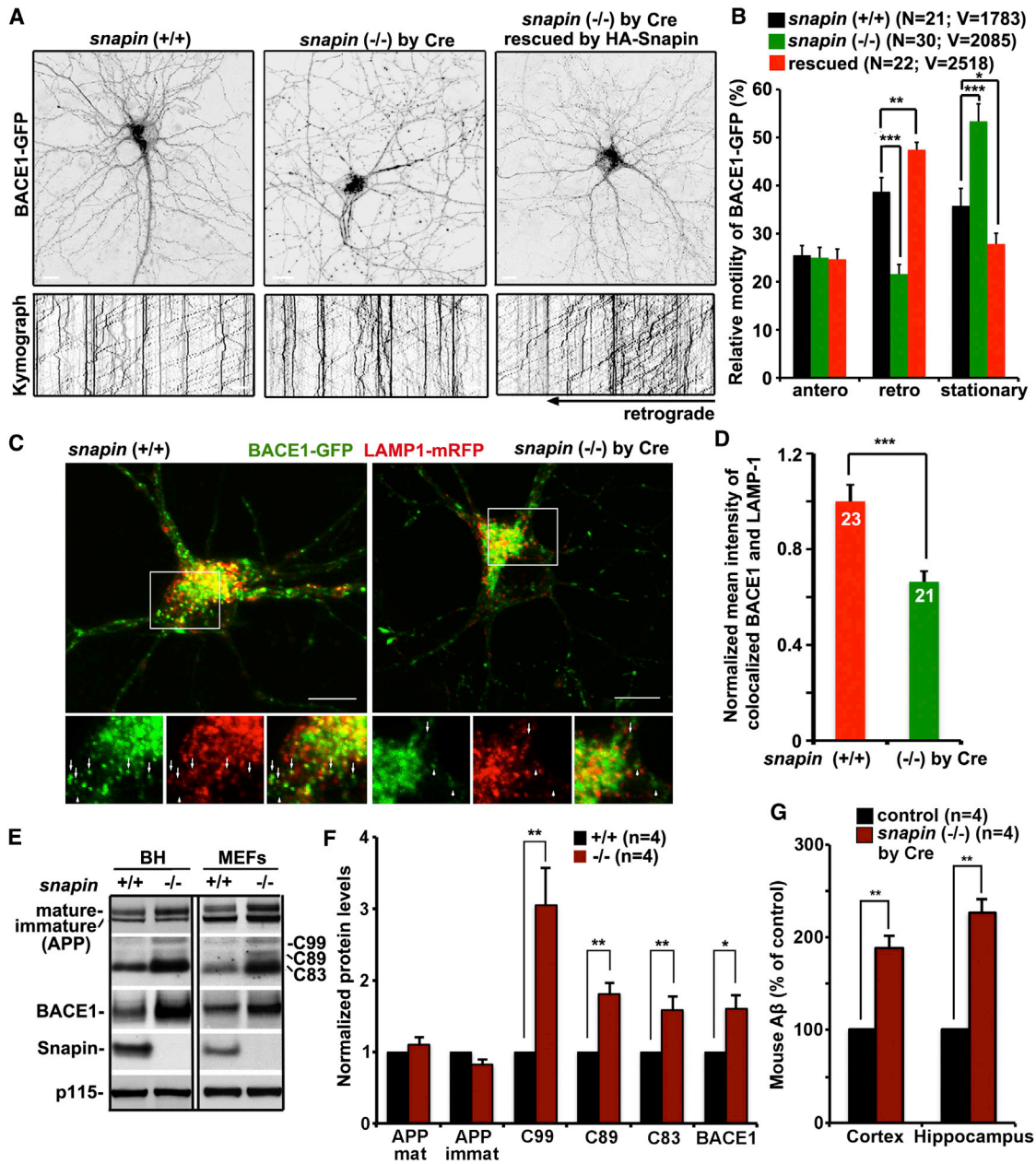
Figure 3. Snapin-DIC Interaction Regulates APP Processing

(A and B) Representative images and kymographs (A) and quantitative analysis (B) showing relative distribution and motility of BACE1 in cortical neurons (12–13 DIV) from homozygous *snapin flox* mice, or expressed with Cre, or rescued *snapin*-deficient neurons. antero, anterograde; retro, retrograde.

(C and D) Representative images (C) and quantitative analysis (D) showing reduced lysosomal targeting of BACE1 in *snapin*-deficient neurons. Cortical neurons cultured from *snapin flox* mice were cotransfected with BACE1-GFP and LAMP-1-mRFP, or with Cre at 6 DIV and imaged at 12–13 DIV. Bottom panels (C) are close-up views of the boxed areas. Arrows point to vesicular structures containing both BACE1 and LAMP-1, whereas arrowheads mark BACE1 puncta unlabeled by LAMP-1. Normalized mean intensity for colocalization reflects relative BACE1 targeting to lysosomes in soma.

(E and F) Representative blots (E) and quantitative analysis (F) showing enhanced APP processing by deleting *snapin* in mouse brains and MEFs. A total of 20 μg of brain homogenates (BH) and MEF lysates was sequentially detected on the same membrane with antibodies as indicated. Change in protein levels from BH was normalized by p115. Data were collected from four independent repeats. mat, mature; imat, immature.

(G) Increased mouse Aβ levels in the cerebral cortex and hippocampus of 1-month-old conditional *snapin*-deficient mice compared with their littermate controls. Cerebral cortex and hippocampus were homogenized with guanidine HCl extraction buffer, and the homogenates were analyzed by ELISA for mouse Aβ40 levels (n = 4 for each of the genotypes).

Data were quantified from a total number of axonal BACE1 cargos (V) from a total number of neurons (N) as indicated in parentheses (B) or from a total number of neurons (N) indicated on the top of bars (D) in more than three experiments. Scale bars represent 10 μm. Error bars represent SEM. Student's t test: ***p < 0.001; **p < 0.01; *p < 0.05. See also Figure S3 and Movies S5, S6, and S7.
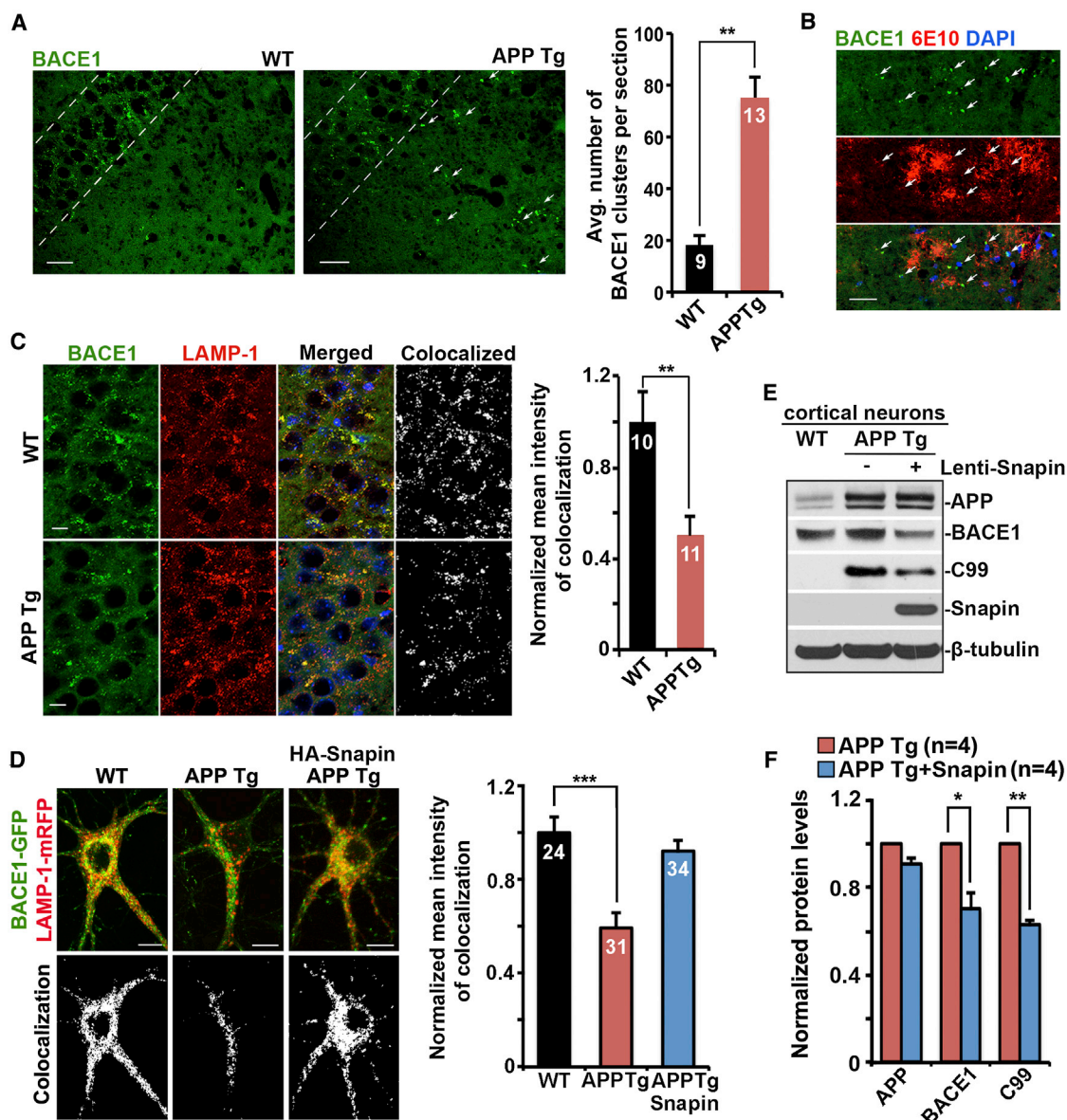
Figure 4. Snapin Reduces APP Processing

(A) BACE1 clustering (arrows) in distal processes of hippocampal CA3 regions in hAPP Tg mice. The number of BACE1 clusters per section (320 × 320 μm) was quantified. Avg., average.

(B) Increased association of BACE1 with 6E10-labeled APP, C99, and Aβ deposits within swollen/dystrophic neurites in the hippocampal regions of hAPP Tg mice.

(C) Impaired BACE1 targeting to lysosomes in the soma of hippocampal CA3 regions in hAPP Tg mice.

(D) Impaired lysosomal targeting of BACE1 in the soma of hAPP Tg neurons coexpressing BACE1-GFP and LAMP-1-mRFP, which was rescued by Snapin overexpression.

(E and F) Overexpressing Snapin decreased the levels of BACE1 and APP-C99 in hAPP mutant neurons. Neurons were infected with Lenti-Snapin at 6–7 DIV, followed by collection of cell lysates at 11–12 DIV. A total of 40 μg of lysates was sequentially detected on the same membrane with antibodies as indicated. Changes in protein levels were normalized by β-tubulin and to those of noninfected hAPP mutant neurons. Data were collected from four independent repeats.

Scale bars represent 25 μm (A and B) and 10 μm (C and D). Data were quantified from a total number of imaging slice sections (A), imaging fields (C), or neurons (D) indicated on the top of bars from more than three experiments. Error bars represent SEM. Student's t test: ***p < 0.001; **p < 0.01; *p < 0.05. See also Figure S4.

of BACE1 from distal processes to the somatic lysosomes for degradation. In *snapin*-deficient neurons, BACE1 retrograde transport was selectively impaired (Figure 3), resulting in the following major cellular defects: (1) BACE1 was clustered along distal neuronal processes (Figure 3A); (2) BACE1 was retained within late endocytic organelles rather than being delivered to

lysosomes for degradation (Figures 3 and S3); (3) BACE1 and APP-CTFs were increased in neurons and MEFs (Figure 3); and (4) Aβ levels were increased in the cerebral cortex and hippocampus of *snapin*-deficient mouse brains (Figure 3G). These phenotypes could be rescued by reintroducing *snapin* transgenes, but not its L99K mutant defective in DIC binding (Figures 3, S3, and S4). Furthermore, elevated Snapin expression in hAPP mutant neurons reverses the defects in BACE1 retrograde transport and lysosomal degradation, thus reducing APP amyloidogenic processing (Figures 2, 4, and S2). Therefore, Snapin-DIC interaction is one of the primary pathways mediating BACE1 trafficking and turnover in neurons.

Efficient intracellular transport is critical for neuronal function and survival because main synthetic and degradative compartments are located in the soma. Dynein-driven retrograde transport is essential for delivering late endosomal cargo from the cell periphery and distal processes to the soma for lysosomal degradation. A large body of evidence implicates defective axonal transport in AD (Stokin and Goldstein, 2006). The deficits in retrograde transport of BDNF-TrkB signaling endosomes have been recently reported in APP mutant neurons (Poon et al., 2013). Because signaling endosomes are specialized late endocytic organelles (Zhou et al., 2012), it is consistent with our observations of impaired retrograde transport of late endosomes. Our study provides evidence that impaired BACE1 retrograde transport in hAPP mutant cortical neurons compromises its lysosomal degradation, thus enhancing its β secretase activity and Aβ generation.

Recent work by Das et al. (2013) demonstrated that APP and BACE1 are sorted into distinct neuronal organelles in resting states. Synaptic activity induces convergence of APP and BACE1 along the endocytic pathway, thus triggering amyloidogenesis. Our study provided further evidence that APP, C99, and Aβ were accumulated together with BACE1 within late endosomes in dystrophic neurites of hAPP Tg neurons. Given that the amyloidogenic processing of APP occurs preferential in endosomes, our findings provide mechanistic insights into the cellular mechanism underlying the retention of APP and BACE1 within the endocytic system for Aβ generation. Altogether, these results allow us to propose a model in which Snapin-dynein mediates the delivery of BACE1 to lysosomes in the soma for controlling its β secretase activity. Future therapeutic approaches aimed at modulating the Snapin-dynein coupling may help rescue defective BACE1 transport found in AD and thus restrict Aβ production in neurons.

EXPERIMENTAL PROCEDURES

Mouse cortical neuron cultures were prepared from E18–E19 mouse embryos or P0 mouse pups as described (Cai et al., 2010, 2012). Neuron images were acquired on an Olympus FV1000 confocal microscope with a 60× oil-immersion objective by sequential acquisition. For morphological analysis, z stack (eight to ten optical sections) images were acquired by using the same settings below saturation at a resolution of 1,024 × 1,024 pixels (eight bit), and brightest point projections were made. Colocalization and morphometric measurements were performed using NIH ImageJ. Neurons for time-lapse imaging were plated at $1 \times 10^5/cm^2$. BACE1-GFP or YFP-Rab7 and LAMP-1-mRFP were cotransfected at 6–9 DIV and incubated for an additional 72–96 hr. Neurons were incubated in a heated confocal living-cell incubator for at least 6 min

before imaging with a 60× oil-immersion objective lens (N.A. 1.3) on an Olympus FV1000 confocal microscope. Due to distinct microtubule organization in axons and dendrites, only axonal processes were selected for motility analysis.

SUPPLEMENTAL INFORMATION

Supplemental Information includes Supplemental Results, Supplemental Discussion, Supplemental Experimental Procedures, four figures, and seven movies and can be found with this article online at http://dx.doi.org/10.1016/j.celrep.2013.12.008.

REFERENCES

Cai, Q., Lu, L., Tian, J.H., Zhu, Y.B., Qiao, H., and Sheng, Z.H. (2010). Snapin-regulated late endosomal transport is critical for efficient autophagy-lysosomal function in neurons. Neuron *68*, 73–86.

Cai, Q., Zakaria, H.M., Simone, A., and Sheng, Z.H. (2012). Spatial parkin translocation and degradation of damaged mitochondria via mitophagy in live cortical neurons. Curr. Biol. *22*, 545–552.

Das, U., Scott, D.A., Ganguly, A., Koo, E.H., Tang, Y., and Roy, S. (2013). Activity-induced convergence of APP and BACE-1 in acidic microdomains via an endocytosis-dependent pathway. Neuron *79*, 447–460.

Fukumoto, H., Rosene, D.L., Moss, M.B., Raju, S., Hyman, B.T., and Irizarry, M.C. (2004). Beta-secretase activity increases with aging in human, monkey, and mouse brain. Am. J. Pathol. *164*, 719–725.

Ginsberg, S.D., Mufson, E.J., Counts, S.E., Wuu, J., Alldred, M.J., Nixon, R.A., and Che, S. (2010). Regional selectivity of rab5 and rab7 protein upregulation in mild cognitive impairment and Alzheimer's disease. J. Alzheimers Dis. *22*, 631–639.

Haass, C., Koo, E.H., Mellon, A., Hung, A.Y., and Selkoe, D.J. (1992). Targeting of cell-surface beta-amyloid precursor protein to lysosomes: alternative processing into amyloid-bearing fragments. Nature *357*, 500–503.

Hardy, J., and Selkoe, D.J. (2002). The amyloid hypothesis of Alzheimer's disease: progress and problems on the road to therapeutics. Science *297*, 353–356.

Huse, J.T., Pijak, D.S., Leslie, G.J., Lee, V.M., and Doms, R.W. (2000). Maturation and endosomal targeting of beta-site amyloid precursor protein-cleaving enzyme. The Alzheimer's disease beta-secretase. J. Biol. Chem. *275*, 33729–33737.

Jankowsky, J.L., Slunt, H.H., Gonzales, V., Savonenko, A.V., Wen, J.C., Jenkins, N.A., Copeland, N.G., Younkin, L.H., Lester, H.A., Younkin, S.G., and Borchelt, D.R. (2005). Persistent amyloidosis following suppression of Abeta production in a transgenic model of Alzheimer disease. PLoS Med. *2*, e355.

Kang, E.L., Biscaro, B., Piazza, F., and Tesco, G. (2012). BACE1 protein endocytosis and trafficking are differentially regulated by ubiquitination at lysine 501

and the Di-leucine motif in the carboxyl terminus. J. Biol. Chem. *287*, 42867–42880.

Koo, E.H., and Squazzo, S.L. (1994). Evidence that production and release of amyloid beta-protein involves the endocytic pathway. J. Biol. Chem. *269*, 17386–17389.

Lee, S., Sato, Y., and Nixon, R.A. (2011). Lysosomal proteolysis inhibition selectively disrupts axonal transport of degradative organelles and causes an Alzheimer's-like axonal dystrophy. J. Neurosci. *31*, 7817–7830.

Lefort, R., Pozueta, J., and Shelanski, M. (2012). Cross-linking of cell surface amyloid precursor protein leads to increased β-amyloid peptide production in hippocampal neurons: implications for Alzheimer's disease. J. Neurosci. *32*, 10674–10685.

Mucke, L., Masliah, E., Yu, G.Q., Mallory, M., Rockenstein, E.M., Tatsuno, G., Hu, K., Kholodenko, D., Johnson-Wood, K., and McConlogue, L. (2000). High-level neuronal expression of abeta 1-42 in wild-type human amyloid protein precursor transgenic mice: synaptotoxicity without plaque formation. J. Neurosci. *20*, 4050–4058.

Nixon, R.A. (2005). Endosome function and dysfunction in Alzheimer's disease and other neurodegenerative diseases. Neurobiol. Aging *26*, 373–382.

Poon, W.W., Carlos, A.J., Aguilar, B.L., Berchtold, N.C., Kawano, C.K., Zograbyan, V., Yaopruke, T., Shelanski, M., and Cotman, C.W. (2013). β-Amyloid (Aβ) oligomers impair brain-derived neurotrophic factor retrograde trafficking by down-regulating ubiquitin C-terminal hydrolase, UCH-L1. J. Biol. Chem. *288*, 16937–16948.

Prabhu, Y., Burgos, P.V., Schindler, C., Farías, G.G., Magadán, J.G., and Bonifacino, J.S. (2012). Adaptor protein 2-mediated endocytosis of the β-secretase BACE1 is dispensable for amyloid precursor protein processing. Mol. Biol. Cell *23*, 2339–2351.

Sannerud, R., Declerck, I., Peric, A., Raemaekers, T., Menendez, G., Zhou, L., Veerle, B., Coen, K., Munck, S., De Strooper, B., et al. (2011). ADP ribosylation factor 6 (ARF6) controls amyloid precursor protein (APP) processing by mediating the endosomal sorting of BACE1. Proc. Natl. Acad. Sci. USA *108*, E559–E568.

Stokin, G.B., and Goldstein, L.S. (2006). Axonal transport and Alzheimer's disease. Annu. Rev. Biochem. *75*, 607–627.

Takahashi, R.H., Milner, T.A., Li, F., Nam, E.E., Edgar, M.A., Yamaguchi, H., Beal, M.F., Xu, H., Greengard, P., and Gouras, G.K. (2002). Intraneuronal Alzheimer abeta42 accumulates in multivesicular bodies and is associated with synaptic pathology. Am. J. Pathol. *161*, 1869–1879.

Takahashi, R.H., Almeida, C.G., Kearney, P.F., Yu, F., Lin, M.T., Milner, T.A., and Gouras, G.K. (2004). Oligomerization of Alzheimer's beta-amyloid within processes and synapses of cultured neurons and brain. J. Neurosci. *24*, 3592–3599.

Tesco, G., Koh, Y.H., Kang, E.L., Cameron, A.N., Das, S., Sena-Esteves, M., Hiltunen, M., Yang, S.H., Zhong, Z., Shen, Y., et al. (2007). Depletion of GGA3 stabilizes BACE and enhances beta-secretase activity. Neuron *54*, 721–737.

Vassar, R., Kovacs, D.M., Yan, R., and Wong, P.C. (2009). The beta-secretase enzyme BACE in health and Alzheimer's disease: regulation, cell biology, function, and therapeutic potential. J. Neurosci. *29*, 12787–12794.

Wang, C.L., Tang, F.L., Peng, Y., Shen, C.Y., Mei, L., and Xiong, W.C. (2012). VPS35 regulates developing mouse hippocampal neuronal morphogenesis by promoting retrograde trafficking of BACE1. Biol. Open *1*, 1248–1257.

Wu, J., Petralia, R.S., Kurushima, H., Patel, H., Jung, M.Y., Volk, L., Chowdhury, S., Shepherd, J.D., Dehoff, M., Li, Y., et al. (2011). Arc/Arg3.1 regulates an endosomal pathway essential for activity-dependent β-amyloid generation. Cell *147*, 615–628.

Yang, L.B., Lindholm, K., Yan, R., Citron, M., Xia, W., Yang, X.L., Beach, T., Sue, L., Wong, P., Price, D., et al. (2003). Elevated beta-secretase expression and enzymatic activity detected in sporadic Alzheimer disease. Nat. Med. *9*, 3–4.

Zhou, B., Cai, Q., Xie, Y., and Sheng, Z.H. (2012). Snapin recruits dynein to BDNF-TrkB signaling endosomes for retrograde axonal transport and is essential for dendrite growth of cortical neurons. Cell Rep *2*, 42–51.